

## Short PEG-Linkers Improve the Performance of Targeted, Activatable Monoclonal Antibody-Indocyanine Green Optical Imaging Probes

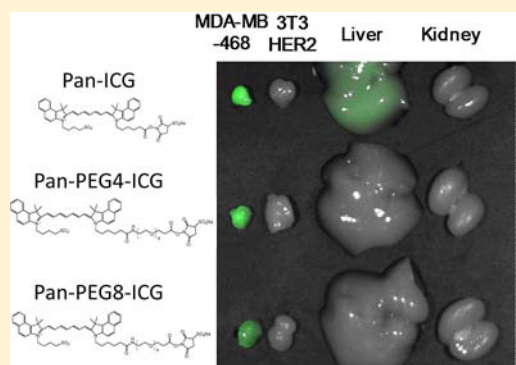
Kohei Sano,<sup>†</sup> Takahito Nakajima,<sup>†</sup> Kiminori Miyazaki,<sup>‡</sup> Yuya Ohuchi,<sup>‡</sup> Takashi Ikegami,<sup>‡</sup> Peter L. Choyke,<sup>†</sup> and Hisataka Kobayashi<sup>\*,†</sup>

<sup>†</sup>Molecular Imaging Program, Center for Cancer Research, National Cancer Institute, National Institutes of Health, Bethesda Maryland 20892, United States

<sup>‡</sup>Dojindo Laboratories, 2025-5 Tabaru Kamimashikigun, Mashikimachi, Kumamoto 861-2202, Japan

### S Supporting Information

**ABSTRACT:** The ability to switch optical imaging probes from the quenched (off) to the active state (on) has greatly improved target to background ratios. The optimal activation efficiency of an optical probe depends on complete quenching before activation and complete dequenching after activation. For instance, monoclonal antibody-indocyanine green (mAb-ICG) conjugates, which are promising agents for clinical translation, are normally quenched, but can be activated when bound to a cell surface receptor and internalized. However, the small fraction of commonly used ICG derivative (ICG-Sulfo-OSu) can bind noncovalently to its mAb and is, thus, gradually released from the mAb leading to relatively high background signal especially in the liver and the abdomen. In this study, we re-engineered a mAb-ICG conjugate, (Panitumumab-ICG) using bifunctional ICG derivatives (ICG-PEG4-Sulfo-OSu and ICG-PEG8-Sulfo-OSu) with short polyethylene glycol (PEG) linkers. Higher covalent binding (70–86%) was observed using the bifunctional ICG with short PEG linkers resulting in less *in vivo* noncovalent dissociation. Panitumumab-ICG conjugates with short PEG linkers were able to detect human epidermal growth factor receptor 1 (EGFR)-positive tumors with high tumor-to-background ratios (15.8 and 6.9 for EGFR positive tumor-to-negative tumor and tumor-to-liver ratios, respectively, at 3 d postinjection).



### INTRODUCTION

Targeted optical probes are becoming increasingly important for endoscopic and surgical guidance.<sup>1,2</sup> Monoclonal antibodies (mAb) are an attractive targeting moiety for optical probes because many of them are already clinically approved and conjugation to a fluorophore can be accomplished without jeopardizing the binding affinity of the mAb. A particular feature of optical imaging probes, as opposed to other molecular imaging probes such as radionuclides, is that they are switchable; i.e., they can be turned off and on as needed.<sup>3,4</sup> This enables high target-to-background ratios (TBRs), improving sensitivity of the optical agent for detection of pathology. Optical imaging can achieve target-specific, activatable imaging by utilizing switchable signaling fluorophores based on a variety of photochemical mechanisms including autoquenching (Hetero-FRET), self-quenching (Homo-FRET),<sup>5</sup> and pH activation (photoinduced energy transfer; PeT).<sup>6</sup>

A particularly attractive activatable optical imaging probe is based on a mAb conjugated to bifunctional indocyanine green (ICG)-derivatives, in which one sulfonic acid is replaced with a carbonic acid which is then used for conjugation with the mAb. Many mAbs are clinically approved and ICG has over 50 years experience of human use as a fluorophore with an excellent safety profile, making the mAb-ICG conjugate highly plausible for

clinical translation. Moreover, its fluorescence emission is in the near-infrared (NIR) where light penetration through tissue is maximal. When conjugated with mAbs, ICG autoquenches as a result of interactions between the ICG and aromatic amino acids on the mAb molecules. Upon degradation of antibodies, as occurs after cellular internalization, ICG is released from the antibodies inducing hetero-FRET and is a relatively efficient light emitter. However, even after intense purification, some proportion of ICG remains noncovalently bound to mAb. Some proportion of noncovalent ICG fraction is gradually released from the mAb into the circulation and is excreted through the biliary system as an ICG monomer, leading to high nonspecific background signals, especially in the liver and the abdomen. Although target tumors can be readily identified due to their prolonged intense signal for several days, this high background signal reduces the target-to-background ratio, especially around the liver and bowel within 24 h after injection. Thus, a major goal of modifying the conjugate chemistry of ICG is to reduce the background signal derived from the noncovalent

**Received:** January 27, 2013

**Revised:** April 20, 2013

**Published:** April 22, 2013

fraction of ICG and increase and prolong the target tumor signal derived from the covalent fraction of ICG.

Here we demonstrate that inserting a short PEG linker between ICG and Sulfo-O-Succinimidyl functional residues results in bifunctional ICG derivatives (ICG-PEG4-Sulfo-OSu and ICG-PEG8-Sulfo-OSu, Figure 1) with more covalent linkage

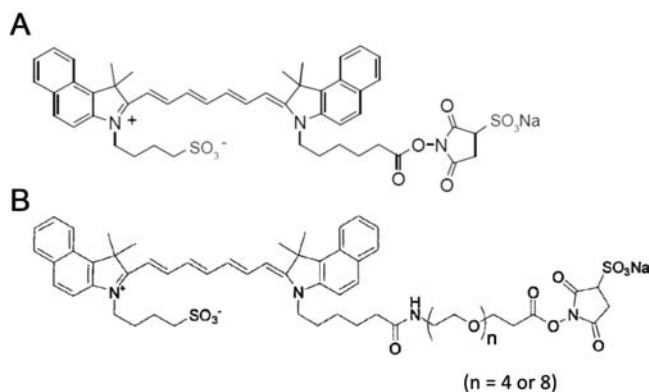


**Figure 1.** Chemical structures of (A) ICG-Sulfo-OSu and (B) ICG-PEG4-Sulfo-OSu ( $n = 4$ ), and ICG-PEG8-Sulfo-OSu ( $n = 8$ ).

between the ICG and mAb. When these bifunctional derivatives are conjugated to an anti-human epidermal growth factor receptor 1 (EGFR) mAb (Panitumumab; Pan), they demonstrate superior target-to-background ratios compared with conventional Pan-ICG conjugates. Herein, we confirm that PEG-spacer results in an increased percentage of covalent binding to mAb, higher stability in serum, *in vitro* cellular uptake, and improved tumor detection with these modified mAb-bifunctional ICG derivatives.

## EXPERIMENTAL PROCEDURES

**Reagents.** Panitumumab (Pan), a fully human IgG<sub>2</sub> mAb directed against the extracellular domain of the human EGFR, was purchased from Amgen (Thousand Oaks, CA). ICG-Sulfo-OSu was purchased from Dojindo Molecular Technologies, Inc. (Rockville, MD). Amino-dPEG<sub>4</sub>-acid and Amino-dPEG<sub>8</sub>-acid were purchased from Quanta BioDesign, Ltd. (Powell, OH). Sulfo-NHS was obtained from Thermo Fisher Scientific Inc. (Yokohama, Japan). All other chemicals used were of reagent grade.

**Synthesis of ICG-PEG4 Acid (1).** ICG-Sulfo-OSu (300 mg, 0.34 mmol) and Amino-dPEG<sub>4</sub>-acid (105 mg, 0.40 mmol) in DMF (5 mL) was stirred at room temperature overnight. Chloroform (50 mL) was added to the reaction mixture. The solution was washed with water (30 mL) three times. The organic layer was washed with saturated NaCl solution (30 mL) and dried over Na<sub>2</sub>SO<sub>4</sub>. The solvent was removed *in vacuo* and the residue was purified by silica gel column chromatography using 5% methanol/95% chloroform. Compound 1 was obtained as a green powder (174 mg, 54%); ESI-MS (positive mode) calcd for C<sub>56</sub>H<sub>71</sub>N<sub>3</sub>O<sub>10</sub>S ([M]<sup>+</sup>) 977.49, found 978.

**Synthesis of ICG-PEG4-Sulfo-OSu (2; PEG4-ICG).** *N,N'*-Dicyclohexylcarbodiimide (26 mg, 0.13 mmol) was added at 0 °C to a stirred solution of compound 1 (100 mg, 0.10 mmol) and Sulfo-NHS (26 mg, 0.12 mmol) in DMF (3 mL). The reaction mixture was allowed to reach room temperature overnight. Ethyl acetate was added to the reaction mixture and the precipitation was filtered off. The solvent was removed *in vacuo* and the residue was purified by silica gel column chromatography using 20%

methanol/80% chloroform. Compound 2 was obtained as a green powder (62.0 mg, 52%); ESI-MS (positive mode) calcd for C<sub>60</sub>H<sub>73</sub>N<sub>4</sub>Na<sub>2</sub>O<sub>15</sub>S<sub>2</sub> ([M+2Na]<sup>+</sup>) 1199.43, found 1200. <sup>1</sup>H NMR (300 MHz, DMSO-*d*<sub>6</sub>) 8.20 (d, 2H), 8.03–8.00 (m, 6H), 7.83–7.62 (m, 5H), 7.50 (m, 2H), 6.61–6.28 (m, 3H), 6.39 (d, 1H), 5.55 (d, 1H), 4.21 (m, 4H), 3.93 (m, 1H), 3.70 (m, 4H), 3.47 (s, 16H), 3.14 (m, 2H), 2.07 (t, 2H), 1.90 (s, 12H), 1.80–1.68 (m, 4H), 1.63–1.41 (m, 4H), 1.27–1.19 (m, 2H), 1.13–1.05 (m, 2H).

**Synthesis of ICG-PEG8 Acid (3).** ICG-Sulfo-OSu (400 mg, 0.43 mmol) and Amino-dPEG<sub>8</sub>-acid (232 mg, 0.53 mmol) in DMF (7 mL) was stirred at room temperature overnight. Chloroform (70 mL) was added to the reaction mixture. The solution was washed with water (40 mL) twice. The organic layer was washed with saturated NaCl solution (30 mL), and dried over Na<sub>2</sub>SO<sub>4</sub>. The solvent was removed *in vacuo* and the residue was purified by silica gel column chromatography using 5% methanol/95% chloroform. Compound 3 was obtained as a green powder (155 mg, 31%); ESI-MS (negative mode) calcd for C<sub>64</sub>H<sub>86</sub>N<sub>3</sub>O<sub>14</sub>S ([M-H]<sup>-</sup>) 1153.59, found 1152.53.

**Synthesis of ICG-PEG8-Sulfo-OSu (4; PEG8-ICG).** *N,N'*-Dicyclohexylcarbodiimide (34 mg, 0.16 mmol) was added at 0 °C to a stirred solution of compound 3 (95 mg, 0.082 mmol) and Sulfo-NHS (35 mg, 0.16 mmol) in DMF (3 mL). After the reaction mixture was stirred at 0 °C overnight, *N,N'*-dicyclohexylcarbodiimide (34 mg, 0.16 mmol) and Sulfo-NHS (35 mg, 0.16 mmol) were added to the reaction mixture, which was stirred at 4 °C for 2 days. The dicyclohexylurea was removed by filtration and the filtrate was concentrated. Diethyl ether was added to the residue and the precipitation was filtered off. Compound 4 was obtained as a green powder (138 mg, 83%); ESI-MS (positive mode) calcd for C<sub>68</sub>H<sub>89</sub>N<sub>4</sub>Na<sub>2</sub>O<sub>19</sub>S<sub>2</sub><sup>+</sup> ([M+2Na]<sup>+</sup>) 1375.54, found 1375.40. <sup>1</sup>H NMR (300 MHz, DMSO-*d*<sub>6</sub>) 8.25 (d, 2H), 8.06–8.03 (m, 6H), 7.84–7.62 (m, 5H), 7.49 (m, 2H), 6.64–6.50 (m, 3H), 6.40 (d, 1H), 5.57 (d, 1H), 4.20 (m, 4H), 3.95 (m, 1H), 3.69 (m, 4H), 3.48 (s, 30H), 3.15 (m, 2H), 2.07 (t, 2H), 1.91 (s, 12H), 1.79–1.69 (m, 4H), 1.62–1.40 (m, 4H), 1.26–1.18 (m, 2H), 1.13–1.02 (m, 2H).

**Measurement of the Lipophilicity of ICG, PEG4-ICG, and PEG8-ICG.** To evaluate the lipophilicity of ICG derivatives, the partition coefficient (logP) was determined. ICG derivative (50 nmol) was mixed with 1 mL each of 1-octanol and 0.1 mol/L phosphate buffer (pH 7.4) in a test tube. Three tubes were used for each condition. The tubes were shaken intensely (3 × 1 min) and incubated for 20 min at room temperature, and the whole process was repeated twice to ensure that the reaction had reached equilibrium. Then, the concentration of ICG derivatives was measured by absorption with the UV-vis system after 4-fold dilution with 1-octanol or phosphate buffer. The distribution ratios were determined as the logarithm value of the octanol-to-buffer ratio (logP).

**Synthesis of ICG Derivatives Conjugated Antibodies.** Panitumumab (1 mg, 6.8 nmol) was incubated with ICG-Sulfo-OSu (22.3 μg, 24.0 nmol), ICG-PEG4-Sulfo-OSu (20.2 μg, 17.1 nmol), or ICG-PEG8-Sulfo-OSu (46.4 μg, 34.2 nmol) in 0.1 M Na<sub>2</sub>HPO<sub>4</sub> (pH 8.6) at room temperature for one hour, followed by the purification with a size exclusion column (PD-10; GE Healthcare, Piscataway, NJ). The concentrations of ICG were calculated by measuring the absorption with a UV-vis system (8453 Value UV-vis system; Agilent Technologies, Santa Clara, CA) to confirm the number of fluorophore molecules conjugated to each antibody molecule. The protein concentration was also determined by measuring the absorption at 280 nm with a UV-

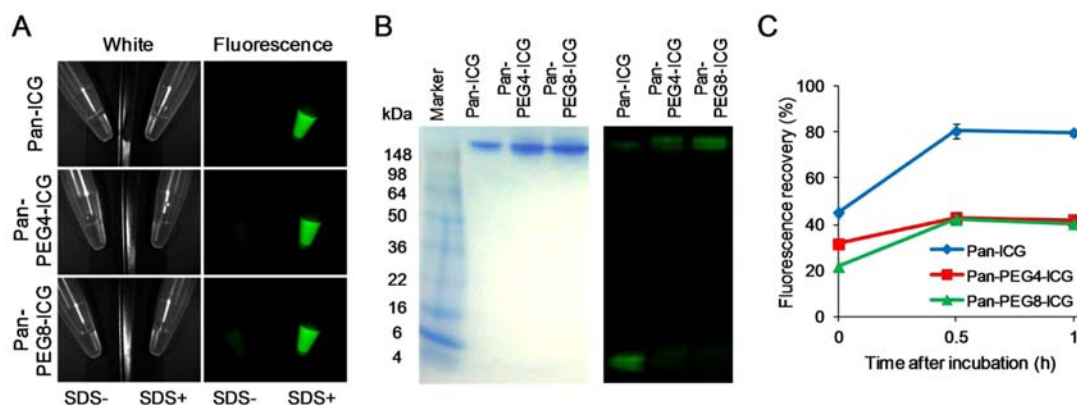


**Figure 2.** (A) Quenched (left) and chemically dequenched (right) Pan-ICG, Pan-PEG4-ICG, and Pan-PEG8-ICG. Dequenched conjugates show increased fluorescence signal shown in green. (B) Validation of the covalent binding of ICG to antibody by SDS-PAGE (left: Colloidal Blue staining, right: fluorescence). (C) Stability of probes in mouse serum. Fluorescence recovery was calculated by the following equation: (Fluorescence signal in mouse serum-Fluorescence signal in PBS)/(Fluorescence signal in SDS/PBS-Fluorescence signal in PBS)  $\times$  100. Data are presented as mean  $\pm$  s.e.m.

vis system. The number of ICG per antibody was adjusted to 1.1–1.4 for each probe. As a quality control for each conjugate, we performed sodium dodecyl sulfate-polyacrylamide gel electrophoresis (SDS-PAGE) as previously described.<sup>7</sup> Each conjugate was separated by SDS-PAGE with a 4–20% gradient polyacrylamide gel (Life technologies, Gaithersburg, MD). A standard marker was used as a protein molecular weight marker. After electrophoresis at 100 V for 5 min followed by 80 V for 2 h, the gel was imaged with a Pearl Imager (LI-COR Biosciences using the 800 nm fluorescence channel). The gel was stained with Colloidal Blue staining to determine the molecular weight of conjugates.

**Determination of Quenching Capacity in Vitro.** The quenching capacity of each conjugate was investigated by denaturation with 1% SDS as described previously.<sup>8</sup> Briefly, the conjugates were incubated with 1% SDS in PBS for 15 min at room temperature. As a control, the samples were incubated in PBS. The change in fluorescence signal intensity of ICG was investigated with an *in vivo* imaging system (Maestro, CRi Inc., Woburn, MA) using a 710 to 760 nm excitation filter and an 800 nm long-pass emission filter.

**Stability in Mouse Serum.** Each probe (37.5  $\mu$ g in PBS) was incubated in mouse serum (50  $\mu$ L) for 0, 0.5, and 1 h at 37  $^{\circ}$ C, followed by imaging with a Pearl Imager. 1% SDS was added to each probe to dequench. Fluorescence recovery in mouse serum was calculated by the following equation: (Fluorescence signal in mouse serum-Fluorescence signal in PBS)/(Fluorescence signal in SDS-Fluorescence signal in PBS)  $\times$  100.

**Cell Culture.** The EGFR+ breast cancer cell line, MDA-MB-468, and EGFR- cell line, NIH/3T3 (3T3/HER2), were used. Both cell lines were grown in RPMI 1640 (Life Technologies) containing 10% fetal bovine serum (Life Technologies), 0.03% L-glutamine, 100 units/mL penicillin, and 100  $\mu$ g/mL streptomycin in 5% CO<sub>2</sub> at 37  $^{\circ}$ C.

**Fluorescence Microscopy Studies.** MDA-MB-468 cells (1  $\times$  10<sup>4</sup>) were plated on a covered glass-bottomed culture well and incubated for 16 h. Pan-ICG, Pan-PEG4-ICG, and Pan-PEG8-ICG (10  $\mu$ g/mL) were then added to MDA-MB-468 cells, respectively. The cells were incubated for either one or six hours followed by washing once with PBS, and fluorescence microscopy was performed using an Olympus X81 microscope (Olympus America, Inc., Melville, NY) equipped with the following filters: excitation wavelength 672.5–747.5 nm and emission wavelength 765–855 nm for ICG. Transmitted light

differential interference contrast images were also acquired. To validate the specific binding of the antibody, 3T3/HER2 cells (EGFR negative cells) were used as a control.

**Tumor Model.** All procedures were carried out in compliance with the Guide for the Care and Use of Laboratory Animal Resources (1996), National Research Council, and approved by the Animal Care and Use Committee in the National Cancer Institute. Six- to eight-week-old female homozygote athymic nude mice were purchased from Charles River (NCI-Frederick, Frederick, MD). During the procedure, mice were anesthetized with isoflurane. MDA-MB-468 cells (2  $\times$  10<sup>6</sup>) and 3T3/HER2 cells (2  $\times$  10<sup>6</sup>) were injected into right and left mammary pads, respectively. Mice were imaged when tumors grew to about 5 mm as reported previously.<sup>9</sup>

**In Vivo Imaging Studies Targeting for EGFR.** Each probe (Pan-ICG, Pan-PEG4-ICG, and Pan-PEG8-ICG, each 100  $\mu$ g/100  $\mu$ L PBS) was injected via tail vein into tumor-bearing mice (MDA-MB-468 and 3T3/HER2-controls). The mice were anesthetized with 1.5% isoflurane, and fluorescence imaging was obtained over three days with a Pearl Imager (LI-COR) using the 800 nm fluorescence channel. Mice were sacrificed with carbon dioxide immediately after the final imaging session. The tumors were excised and *ex vivo* imaging was performed using the Pearl Imager.

**Statistical Analysis.** Quantitative data were expressed as mean  $\pm$  s.e.m. Means were compared using two-way repeated measures ANOVA followed by the Bonferroni test. *P*-value of <0.05 was considered statistically significant.

## RESULTS

**Lipophilicity of ICG Derivatives.** The partition coefficients of ICG, PEG4-ICG, and PEG8-ICG were obtained to determine the lipophilicity. The resulting logP values (higher values indicating higher lipophilicity) were 1.81  $\pm$  0.06, 0.64  $\pm$  0.06, and -0.03  $\pm$  0.02 for ICG, PEG4-ICG, and PEG8-ICG, respectively. Short PEG linkers successfully reduced the lipophilicity of ICG.

**Characterization of Dye Conjugated Antibodies.** By adding 1% SDS to dye-conjugated antibodies, the following dequenching capacities were observed: 15.1-, 10.2-, and 6.7-fold for Pan-ICG, Pan-PEG4-ICG, and Pan-PEG8-ICG, respectively (Figure 2A). As defined by SDS-PAGE, the fractions of covalently bound ICG to panitumumab were 21.8%, 70.9%,



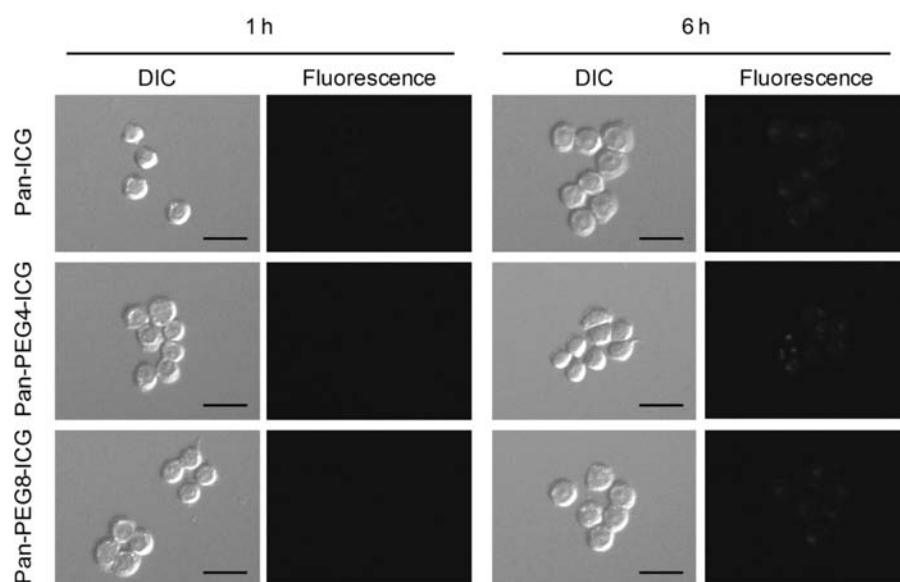


**Figure 3.** Fluorescence microscopy studies. MDA-MB-468 and 3T3/HER2 cells were incubated with Pan-ICG, Pan-PEG4-ICG, and Pan-PEG8-ICG, respectively, for one or six hours. Scale bar indicates 100  $\mu\text{m}$ . The intense fluorescence signals were detected by each probe at 6 hr especially within the tumor cells of MDA-MB-468, not 3T3/HER2.

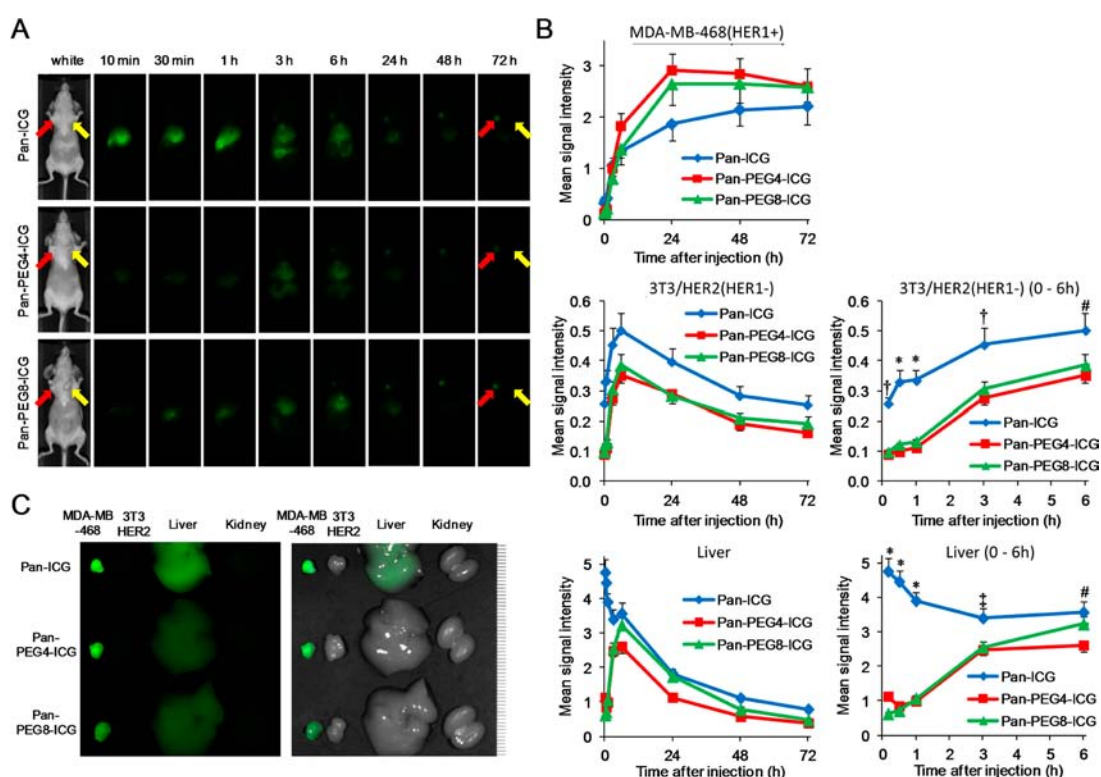


**Figure 4.** (A) *In vivo* serial fluorescence images of MDA-MB-468 (right breast; EGFR positive) and 3T3/HER2 tumor (left breast; EGFR negative control) bearing mice injected with Pan-ICG, Pan-PEG4-ICG, or Pan-PEG8-ICG. (B) Dynamic changes of signal intensity in MDA-MB-468, 3T3/HER2, and liver are depicted. Data are means  $\pm$  s.e.m. ( $n = 5$ ). \* $P < 0.05$ , † $P < 0.01$ , \* $P < 0.0001$  vs Pan-PEG4-ICG and Pan-PEG8-ICG group. # $P < 0.01$  vs Pan-PEG4-ICG. (C) *Ex vivo* fluorescence images of MDA-MB-468, 3T3/HER2, liver, and kidneys obtained 72 h after injection of probes are shown. Smallest scale bar indicates 1 mm.

and 85.5% for Pan-ICG, Pan-PEG4-ICG, and Pan-PEG8-ICG, respectively (Figure 2B). The dissociated ICG was observed in the small molecule fraction. The conjugation ratio of ICG to mAb ( $>1$ ) was higher than previous studies which ranged from 0.3 to 0.5. Pan-ICG showed a 79.7% increase in fluorescence intensity 1 h after incubation in mouse serum (Figure 2C),

compared with Pan-PEG4-ICG and Pan-PEG8-ICG (41.8% and 40.4%, respectively).

**In Vitro Microscopy Studies.** Microscopy studies (Figure 3) demonstrated initial fluorescence was low at 1 h but increased substantially at 6 h for all conjugates. These results suggest that each conjugate is activated after internalization and lysosomal

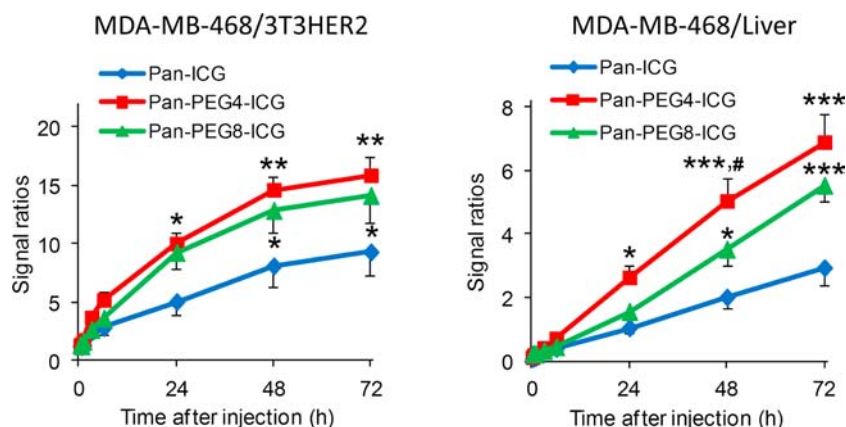


**Figure 5.** MDA-MB-468 tumor to 3T3/HER2 tumor (left) or liver (right) signal intensity ratios. PEGylation of ICG could improve the targeted tumor to background ratios. Pan-PEG4-ICG provided highest ratios compared Pan-ICG and Pan-PEG8-ICG. \* $P < 0.05$ , \*\* $P < 0.001$ , \*\*\* $P < 0.0001$  vs Pan-ICG group. # $P < 0.05$  vs Pan-PEG8-ICG group.

processing (Supporting Information Figure S1), which leads to complete dequenching by 1 h. No signal was detected in EGFR negative 3T3/HER2 cells regardless of probe.

**In Vivo Fluorescence Dynamic Imaging Study.** Figure 4 shows the imaging and quantitative assessment of tumor-bearing mice (MDA-MB-468 and 3T3/HER2) administered Pan-ICG, Pan-PEG4-ICG, or Pan-PEG8-ICG, using the 800 nm fluorescence channel of the fluorescence camera. EGFR positive tumors (MDA-MB-468) were observed by 6 h and at all later time points (no significant difference between groups), while minimal fluorescence signal was detected in control tumors (3T3/HER2) at all time points (Figure 4A,B). Pan-ICG, unlike Pan-PEG4-ICG and Pan-PEG8-ICG, exhibited significantly intense signals in the liver just after injection of probes (10 min to 1 h), and the ICG was gradually excreted into the intestine via the biliary tract (Figure 4A,B). At 3 h post injection, Pan-PEG4-ICG and Pan-PEG8-ICG also depicted the liver because of physiological metabolism of the antibody, while highest background signal was observed at all time points when Pan-ICG was employed (Figure 4A,B). While MDA-MB-468 tumors were clearly identified with ICG-specific fluorescence signal, no 3T3/HER2 specimen produced a detectable signal (Figure 4C). MDA-MB-468-to-3T3/HER2 or -to-liver signal intensity ratios were increased with time for each probe (Figure 5). Among them, Pan-PEG4-ICG achieved the highest ratios (15.8 and 6.9 for MDA-MB-468-to-3T3/HER2 and MDA-MB-468-to-liver ratios at 3 days). There was no difference in biodistribution of nonconjugated ICG, PEG4-ICG, and PEG8-ICG (Supporting Information Figure S2).

## DISCUSSION

PEGylation is a well-known method for improving both the *in vivo* pharmacokinetics of various biologically interesting proteins or peptides and their *in vivo* stability.<sup>10,11</sup> PEGylation has also been applied to modify pharmacokinetic properties of small molecules including radiopharmaceuticals by modulating their hydrophobicity.<sup>12,13</sup> In this study, the addition of short PEGs to the linker between ICG and mAbs increased the percentage of covalent binding of ICG to mAb even while using higher conjugation ratios of ICG to mAb probably because of increased hydrophilicity. In contrast, the quenching capacity of conjugated ICG was decreased in proportion to the length of the PEG chain probably due to the increased distance between the ICG and aromatic amino acids on mAb molecules.<sup>8</sup> We confirmed

quenching capacities of 10.2 and 6.7 for Pan-PEG4-ICG and Pan-PEG8-ICG, respectively, which was, nonetheless, high enough to reduce background fluorescence signals. Furthermore, stability testing in mouse plasma and during *in vivo* imaging studies revealed minimal release of free ICG from Pan-PEG4-ICG and Pan-PEG8-ICG producing more quenching compared to the original ICG-Sulfo-OSu conjugated mAbs which demonstrated high uptake in the liver and high background signals in the abdomen due to noncovalently bound original ICG-Sulfo-OSu. In order to determine an appropriate ICG derivative, which shows optimal signal-to-background ratios, the balance between proximity of ICG to mAb molecules and covalent conjugation ratios should be considered. Pan-PEG4-ICG exhibited greater quenching than Pan-PEG8-ICG regardless of a little higher proportion of noncovalently conjugated ICG on Pan-PEG4-ICG.

Among the NIR dyes, ICG is a fluorescence dye that has long been approved by the FDA for clinical use in retinal angiography and for intraoperative assessment of liver function.<sup>14,15</sup> A bifunctional ICG-derivative is highly quenchable, regardless of whether it is covalently or noncovalently bound to a carrier mAb, and can turn the probe “on” only at the target tissue by employing signal activation mechanisms.<sup>16,17</sup> On the other hand, the signal emanating from “always-on” probes (including IRDye700 and IRDye800-labeled probes) reflects their bio-distribution but also results in high background signal. We modified the linker of ICG-Sulfo-OSu with short PEGs but did not alter the core structure of ICG.

This conjugate has several advantages over other *de novo* synthesized optical probes. First ICG has been used clinically for many years. Therapeutic mAbs targeting several receptors including EGFR and HER2 have recently been approved by the FDA, e.g., panitumumab is now in clinical use. Finally, the biocompatibility of PEG is well-known and has been widely used in clinical products.<sup>18,19</sup> Of course, formal safety studies of the final conjugates will be required prior to approval for human use, but it is encouraging that each component has a favorable toxicity profile.

A potential alternative for activatable *in vivo* imaging is the use of fluorescent proteins, which are excellent endogenous fluorescence emitters for depicting various biological processes both *in vitro* and *in vivo*.<sup>20,21</sup> A recently reported alternative technology to this method is tumor-specific imaging using telomerase promoter-regulated expression of fluorescent pro-

teins, which are induced with adenovirus-mediated gene transfection *in vivo*.<sup>22,23</sup> These technologies might have unique clinical benefits for detecting cancer based on biological features. However, for common medical application, the requirement that fluorescence proteins are transduced by virus-mediated *in vivo* gene transfection makes this approach less practical.

In conclusion, we synthesized bifunctional ICG derivatives with short PEG linkers and successfully conjugated them to panitumumab, an anti-EGFR monoclonal antibody. ICG with PEG linkers significantly increased the percentage of covalent binding of ICG to antibody and the conjugates were able to specifically depict positive tumors with high tumor-to-background ratios especially for lesions in or near the liver compared with the original mAb-ICG conjugate without short PEG linkers.

## ■ ASSOCIATED CONTENT

### ■ Supporting Information

Structures of intermediate products, intracellular coregistration of ICG and Lysotracker, and biodistribution of ICG, PEG4-ICG, and PEG8-ICG in normal mice. This material is available free of charge via the Internet at <http://pubs.acs.org>.

## ■ AUTHOR INFORMATION

### Corresponding Author

\*Phone: 301-451-4220. Fax: 301-402-3191. E-mail: Kobayash@mail.nih.gov.

### Notes

The authors declare no competing financial interest.

## ■ ACKNOWLEDGMENTS

This research was supported by the Intramural Research Program of the National Institutes of Health, National Cancer Institute, Center for Cancer Research. We would like to thank T. Ido and M. Ishiyama (Dojindo Molecular Technologies, Inc.) for their support.

## ■ REFERENCES

- (1) Frangioni, J. V. (2008) New technologies for human cancer imaging. *J. Clin. Oncol.* 26, 4012–4021.
- (2) Wallace, M. B., and Kiesslich, R. (2010) Advances in endoscopic imaging of colorectal neoplasia. *Gastroenterology* 138, 2140–2150.
- (3) Kobayashi, H., Longmire, M. R., Ogawa, M., and Choyke, P. L. (2011) Rational chemical design of the next generation of molecular imaging probes based on physics and biology: mixing modalities, colors and signals. *Chem. Soc. Rev.* 40, 4626–4648.
- (4) Kobayashi, H., Ogawa, M., Alford, R., Choyke, P. L., and Urano, Y. (2010) New strategies for fluorescent probe design in medical diagnostic imaging. *Chem. Rev.* 110, 2620–2640.
- (5) Bremer, C., Tung, C. H., and Weissleder, R. (2001) *In vivo* molecular target assessment of matrix metalloproteinase inhibition. *Nat. Med.* 7, 743–748.
- (6) Urano, Y., Asanuma, D., Hama, Y., Koyama, Y., Barrett, T., Kamiya, M., Nagano, T., Watanabe, T., Hasegawa, A., Choyke, P. L., and Kobayashi, H. (2009) Selective molecular imaging of viable cancer cells with pH-activatable fluorescence probes. *Nat. Med.* 15, 104–109.
- (7) Nakajima, T., Mitsunaga, M., Bander, N. H., Heston, W. D., Choyke, P. L., and Kobayashi, H. (2011) Targeted, activatable, *in vivo* fluorescence imaging of prostate-specific membrane antigen (PSMA) positive tumors using the quenched humanized J591 antibody-indocyanine green (ICG) conjugate. *Bioconjugate Chem.* 22, 1700–1705.
- (8) Ogawa, M., Kosaka, N., Choyke, P. L., and Kobayashi, H. (2009) *In vivo* molecular imaging of cancer with a quenching near-infrared fluorescent probe using conjugates of monoclonal antibodies and indocyanine green. *Cancer Res.* 69, 1268–1272.
- (9) Sano, K., Mitsunaga, M., Nakajima, T., Choyke, P. L., and Kobayashi, H. (2012) *In vivo* breast cancer characterization imaging using two monoclonal antibodies activatably labeled with near infrared fluorophores. *Breast Cancer Res.* 14, R61.
- (10) Harris, J. M., and Chess, R. B. (2003) Effect of pegylation on pharmaceuticals. *Nat. Rev. Drug Discovery* 2, 214–221.
- (11) Roberts, M. J., Bentley, M. D., and Harris, J. M. (2002) Chemistry for peptide and protein PEGylation. *Adv. Drug Delivery Rev.* 54, 459–476.
- (12) Stephenson, K. A., Chandra, R., Zhuang, Z. P., Hou, C., Oya, S., Kung, M. P., and Kung, H. F. (2007) Fluoro-pegylated (FPEG) imaging agents targeting Abeta aggregates. *Bioconjugate Chem.* 18, 238–246.
- (13) Ono, M., Watanabe, R., Kawashima, H., Cheng, Y., Kimura, H., Watanabe, H., Haratake, M., Saji, H., and Nakayama, M. (2009) Fluoro-pegylated chalcones as positron emission tomography probes for *in vivo* imaging of beta-amyloid plaques in Alzheimer's disease. *J. Med. Chem.* 52, 6394–6401.
- (14) Dzurinko, V. L., Gurwood, A. S., and Price, J. R. (2004) Intravenous and indocyanine green angiography. *Optometry* 75, 743–755.
- (15) Sakka, S. G. (2007) Assessing liver function. *Curr. Opin. Crit. Care* 13, 207–214.
- (16) Weissleder, R., Tung, C. H., Mahmood, U., and Bogdanov, A., Jr. (1999) *In vivo* imaging of tumors with protease-activated near-infrared fluorescent probes. *Nat. Biotechnol.* 17, 375–378.
- (17) Asanuma, D., Kobayashi, H., Nagano, T., and Urano, Y. (2009) Fluorescence imaging of tumors with "smart" pH-activatable targeted probes. *Methods Mol. Biol.* 574, 47–62.
- (18) Johnson, A. J., Karparkin, M. H., and Newman, J. (1971) [Clinical investigation of intermediate- and high-purity antithrombotic factor (factor VIII) concentrates]. *Br. J. Haematol.* 21, 21–41.
- (19) Zalipsky, S. (1995) Functionalized poly(ethylene glycol) for preparation of biologically relevant conjugates. *Bioconjugate Chem.* 6, 150–165.
- (20) Kishimoto, H., Urata, Y., Tanaka, N., Fujiwara, T., and Hoffman, R. M. (2009) Selective metastatic tumor labeling with green fluorescent protein and killing by systemic administration of telomerase-dependent adenoviruses. *Mol. Cancer Ther.* 8, 3001–3008.
- (21) Kishimoto, H., Aki, R., Urata, Y., Bouvet, M., Momiyama, M., Tanaka, N., Fujiwara, T., and Hoffman, R. M. (2011) Tumor-selective, adenoviral-mediated GFP genetic labeling of human cancer in the live mouse reports future recurrence after resection. *Cell Cycle* 10, 2737–2741.
- (22) Kishimoto, H., Zhao, M., Hayashi, K., Urata, Y., Tanaka, N., Fujiwara, T., Penman, S., and Hoffman, R. M. (2009) *In vivo* internal tumor illumination by telomerase-dependent adenoviral GFP for precise surgical navigation. *Proc. Natl. Acad. Sci. U. S. A.* 106, 14514–14517.
- (23) Bouvet, M., and Hoffman, R. M. (2011) Glowing tumors make for better detection and resection. *Sci. Transl. Med.* 3, 110fs110.